RSC Advances

PAPER

View Article Online
View Journal | View Issue

Cite this: *RSC Adv.*, 2014, **4**, 4856

Localized *in situ* polymerization on carbon nanotube surfaces for stabilized carbon nanotube dispersions and application for cobalt(II) removal

Shubin Yang,[ab] Dadong Shao,[b] Xiangke Wang[b] and Masaaki Nagatsu*[a]

Received 15th November 2013
Accepted 2nd December 2013

DOI: 10.1039/c3ra46701e

www.rsc.org/advances

We demonstrate a two-step *in situ* polymerization method to develop localized polymer coatings on the surface of carbon nanotubes (CNTs). CNTs show good chemical stability, relatively large specific area, porous and layered nanosized structures. However, difficulties in dispersion quality hinder the practical application of CNT-based composites. Poly(*N*,*N*-dimethylacrylamide) (PNDA) is a well-known soluble polymer and it has been proved to improve the sorption efficiency for some metal ions. With these in mind, the plasma-induced grafting polymer technique is used to improve the adsorption capacity and the dispersion property of CNTs. The synthesized multiwalled CNT/poly(*N*,*N*-dimethylacrylamide) (MWCNT/PNDA) composites are characterized. After attaching the polymer, the MWCNT/PNDA composites show highly stable dispersion in aqueous solutions and good properties in the preconcentration and separation of Co(II) ions from aqueous solutions. Co(II) ion sorption by MWCNT/PNDA composites obeyed the Langmuir model, attributed mainly to a outer-sphere surface sorption probably *via* coordination of Co d-electrons to amide and –O–Co and C=C (π-electrons) bonds.

1. Introduction

Rapid industrialization has led to an increased discharge of wastewater containing heavy metals, which have detrimental effects on the environment and human health. Among all of the heavy metal ions, Co(II) can cause serious health trouble, such as low blood pressure, diarrhea, and bone defects.[1] Thus, the removal of excess Co(II) ions from aqueous solution is of practical meaning for public safety. Many techniques such as sorption, ion exchange, (co)precipitation have been applied to remove Co(II) ions. Among these methods, sorption has been used extensively to remove heavy metal ions from aqueous solutions due to its ease of operation, flexibility and simplicity of design. The main problem of sorption technique is how to enhance its sorption capacity and how to increase its sorption selectivity. Proper adsorbent is supposed to own a high sorption capacity, and moderate separability and it should be affordable.

Carbon nanotubes (CNTs) have attracted considerable scientific interest for their high moduli of elasticity, high aspect ratios, and remarkable mechanical, electrical, thermal, optical and magnetic properties[2] since their discovery by Iijima in 1991.[3] In addition to their good chemical stability, relatively large specific area, hollow and layered nanosized structures, CNTs have been proved to be good candidates as adsorbent.[4] However, the main intrinsic drawback of CNTs is their poor dispersibility in common solvents, making it difficult to explore and understand the chemistry of such material at the molecular level and device applications. There are three main reasons for the poor dispersibility of CNTs: (1) the first is the hydrophobic nature; (2) the second is the strong attractive van der Waals forces, which hold the tube surface attracted to each other; and (3) the third is the extremely high aspect ratios in combination with high flexibilities dramatically, which increases the possibilities for entanglements. Entangled aggregates are difficult to disperse without damaging the nanotubes in different ways. Even after long time ultrasound, CNTs still exist in the form of agglomerated and parallel bundles.[2]

Therefore, it is required not only to have excellent properties but also to stabilize the CNTs dispersion for their application. Researches have been extended to include the surface modification of CNTs to improve the dispersion property and sorption capacity of CNTs.[5–7] Because good dispersion can avoid agglomerating and bundling,[5,8–10] leading to extend of the active surface for adsorption.[11,12] Subsequently, more efficient utilization of the respective adsorption sites could be achieved in the sorbent. And these are very suitable parameters for high-performance adsorbent materials in aqueous solution. The most common technique for enhancing the dispersion property of CNTs is the oxidation of CNTs by chemical modification method to form oxidized CNTs. However, in these processes, CNTs are normally refluxed or sonicated in strong acid that

[a]*Graduate School of Science and Technology, Shizuoka University, 3-5-1 Johoku, Naka-ku, Hamamatsu 432-8561, Japan. E-mail: tmnagat@ipc.shizuoka.ac.jp; Fax: +81-53-4781081; Tel: +81-53-4781081*

[b]*Key Laboratory of Novel Thin Film Solar Cells, Institute of Plasma Physics, Chinese Academy of Sciences, P.O. Box 1126, Hefei 230031, PR China. E-mail: xkwang@ipp.ac.cn; Fax: +86-551-65591310; Tel: +86-551-65593308*

harsh conditions may introduce wall damage of CNTs and cleave them into shorter pieces.[13] Especially, these chemical modification processes are not environmental friendly or time-consuming.

Plasma treatment is an efficient method in the field of surface modifications. In recent years, low-temperature plasma-induced grafting technique has attracted great attention because it is a solvent-free and time-efficient method to introduce a wide range of different functional groups.[14] Plasma grafting functional groups to substance surfaces can enhance the chemical functionality. The research works on plasma-induced grafting technique to improve the adsorption capacity and the dispersion property of materials have profound significance to the environmental pollution management. The MWCNTs can be activated easily in plasma treatment process.[15] The plasma technique has been shown to be effective in the surface modification of CNTs without altering the material bulk properties.[14–17]

Aqueous dispersions of CNTs can be prepared by sonicating CNTs combinations with the aid of polymers, biopolymers, and surfactants.[5] For composite application, one must have both excellent dispersion and excellent interfacial adhesion for efficient stress transfer from CNTs to the polymer matrix. These two issues of poor dispersion and poor interfacial strength between filler and matrix is a persistent problem for composites with pristine nanomaterial fillers.[10,18] Surfactant-free CNTs are desirable since the presence of surfactant may affect the thermal properties, transparency, and mechanical properties of the composites. Therefore, the ability to form polymer coatings on CNT surfaces may address this issue of interfacial strength.[19,20]

Poly(*N*,*N*-dimethylacrylamide) (PNDA) is a well-known soluble polymer with large numbers of amide groups. Due to the coordination, amide groups had been proved to improve the sorption efficiency for some metal ions.[16] Thereby, PNDA has been widely grafted to various adsorbent materials to enhance the dispersion and sorption properties.[21]

Herein, we report a two-step method to synthesize MWCNT/PNDA composites by low-temperature plasma technique in N_2 atmosphere. The prepared MWCNT/PNDA composites were characterized by using scanning electron microscopy (SEM), high resolution transmission electron microscopy (HR-TEM), Raman spectroscopy, X-ray powder diffraction (XRD), Brunauer–Emmett–Teller (BET), X-ray photoelectron spectroscopy (XPS), and thermogravimetric analysis (TGA). The MWCNT/PNDA composites were applied as sorbent to remove Co(II) ions from aqueous solutions. The interaction mechanisms of Co(II) with MWCNT/PNDA composites were discussed in detail.

2. Experimental section

2.1 Materials

All chemicals used were analytical grade. Milli-Q (Millipore, Billerica, MA) water was used in the whole experiments. Stock solution of 60 mg L^{-1} Co(II) was prepared from $Co(NO_3)_2$ in Milli-Q water. MWCNTs were prepared by chemical vapor deposition as previously reported.[9]

2.2 Preparation of MWCNT/PNDA composites

The plasma induced grafting of PNDA on MWCNTs consisted of two-step successive processes: surface activation of MWCNTs and PNDA grafting. The typical synthesis procedure was as follows: Firstly, N_2 plasma pretreatment is expected to activate 0.5 g MWCNTs surface by bond breaking due to N_2-ion bombardment and to increase the reactivity of MWCNTs surfaces in a custom-built grafting reactor with magnetic stirring.[9] After 40 min, 50 mL 960 g L^{-1} N^{-1}, *N*-dimethylacrylamide aqueous solution was immediately injected in the reactor. The mixture was kept at 80 °C with stirring for 5 h. After that, the as-made composite was collected by centrifugation, washed with water, and dried in a vacuum condition at 95 °C. The N_2 plasma ignition occurred at 10 Pa with a power of 100 W, voltage of 940 V, and electrical current of 150 mA.

The proposed mechanisms of N_2 plasma induced grafting PNDA on MWCNTs are shown in Scheme 1. The active nitrogen species (N*) first react with MWCNTs to form active species (–C*) in N_2 plasma discharge process. Then the active species –C* react with the olefin double bond (C=C) of PNDA in the following grafting process. After reacting with the active species (–C*), the C=C positions of PNDA carry active species which can react with other monomers, and induce the polymerization of PNDA. Thus PNDA is polymerized and grafted on the surfaces of MWCNTs. And the MWCNT/PNDA composites are synthesized.

2.3 Sample characterization

The SEM images were obtained with a JEOL JSM-6300F. The HR-TEM image was taken on a JEM-2100F microscope. The crystal structures were analyzed by XRD, equipped with Cu Kα radiation ($\lambda = 0.15406$ nm). The Raman spectra of the samples were mounted by using a LabRam HR Raman spectrometry, excitation at 514.5 nm by Ar^+ laser. The XPS measurements were conducted with a VG Scientific ESCALAB Mark II system. The TGA measurements were examined by using a Shimadzu TGA-50 thermogravimetric analyzer from room temperature to 800 °C with heating rate of 10 °C min^{-1} and an N_2 flow rate of 300 mL min^{-1}. The BET equation was obtained with a BELSORP MINI II. The potentiometric titration of the samples were performed with a Metter Toledo DL50 Automatic Titrator at

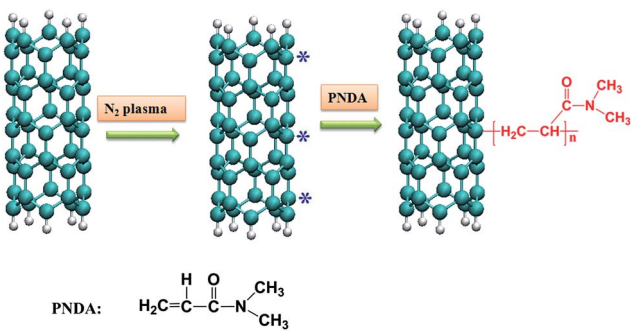

Scheme 1 The synthesis route of MWCNT/PNDA composites by plasma-induced grafting route method.

20 ± 1 °C under N_2 gas conditions, using $NaClO_4$ as background electrolyte and NaOH as titration solution.

2.4 Batch sorption experiment

The adsorption experiments of Co(II) on MWCNT/PNDA were investigated by bath technique in the polyethylene centrifuge tube at $T = 30 \pm 2$ °C. The stock suspensions of MWCNT/PNDA, $NaClO_4$ and Co(II) solutions were added in the tube to achieve the desired concentrations of different components. Adjustment of the pH was undertaken by adding small volumes of 0.01 mol L^{-1} $HClO_4$ or NaOH. After the suspensions were shaken for 24 h, the samples were then separated from the solution using 0.22 μm membrane filters. The Co(II) concentrations were measured by atomic absorption spectrophotometer.

The sorption capacity (C_s, mg g^{-1}) and removal efficiency (E%) were calculated according to the following equations:

$$C_s = \frac{(C_0 - C_e)V}{M} \quad (1)$$

$$E\% = \frac{(C_0 - C_e)}{C_0} \times 100\% \quad (2)$$

where C_0 and C_e represent the initial and equilibrium concentrations (mg L^{-1}) of Co(II) ions, respectively, M is the mass of sorbent (g), V represents the volume of the suspension (L).

3. Results and discussion

3.1 Material characterization

SEM is an effective tool for the morphologic characterization of nanomaterials. Obvious differences of the surface morphology between MWCNTs and MWCNT/PNDA are observed (Fig. 1a and b). The surfaces of MWCNTs (Fig. 1a) are smooth and the CNTs are highly bundled. However, after plasma treatment and attached PNDA polymers, the surfaces (Fig. 1b) become rough. The SEM images show distinctly that some polymers are randomly decorated on the surface of MWCNTs, indicating that MWCNT/PNDA composites are synthesized successfully and poorly crystallized. And the further proof was offered by HR-TEM (Fig. 1c and d). As shown in Fig. 1c and d, the polymer shell and the MWCNTs graphite sheet structure are clearly observed in the HRTEM images.

The XRD patterns of MWCNTs and MWCNT/PNDA are given in Fig. 1e. The main observed intense peaks at $2\theta = 26.1°$ (002) and 43.0° (100) reflections are related to the characteristics of MWCNTs.[22] The XRD patterns of MWCNTs and MWCNT/PNDA are similar to each other, indicating little alteration occurs in the structure of MWCNTs after treated by the N_2 plasma and grafted PNDA polymers. The low temperature plasma treatment only occurs on the surfaces of MWCNTs and does not obviously destroy the framework of MWCNTs.

The visual appearance of the dispersions is drastically different between MWCNTs and MWCNT/PNDA in aqueous solutions (Fig. 1e). In contrast to MWCNTs, MWCNT/PNDA is easily dispersed in aqueous solution. It is necessary to notice that MWCNTs form agglomeration even after 30 min ultrasound (bottle A), showing poor dispersion in aqueous solutions. However, after coating PNDA polymers by the plasma treatment, a black macroscopic homogenous dispersion (B) is obtained. The MWCNT/PNDA homogeneous suspensions could still keep stable even after 2 months of aging time. And the suspensions of MWCNT/PNDA composites can be easy separated from the liquid phase by membrane filters or centrifuging at 10 000 rpm for about 30 minutes. The fact of improving the dispersion of MWCNT/PNDA composites could be due to the formation of amide and oxygen-containing functional groups, which protects the MWCNT/PNDA composites from van der Waals aggregation in scenarios. In addition, we highlight the dispersion of material in aqueous solution in our work. Because good dispersion of the sorbent leads to extend of the active surface for adsorption. And it is a very suitable parameter for high-performance adsorbent materials in aqueous solution. These results evidently indicate the polymerization technique is successful and the MWCNT/PNDA composites with excellent dispersion, long-term stability would serve as an effective material for sorbent.

Raman spectroscopy technique shows a high sensitivity to the disorder structure on various carbon material surfaces.[2] The Raman spectra of MWCNTs and MWCNT/PNDA presented in Fig. 1f are similar to each other. Combined with the SEM and XRD results, the plasma treatment do not seem to obviously damage the integrity of MWCNT structure. The peak near

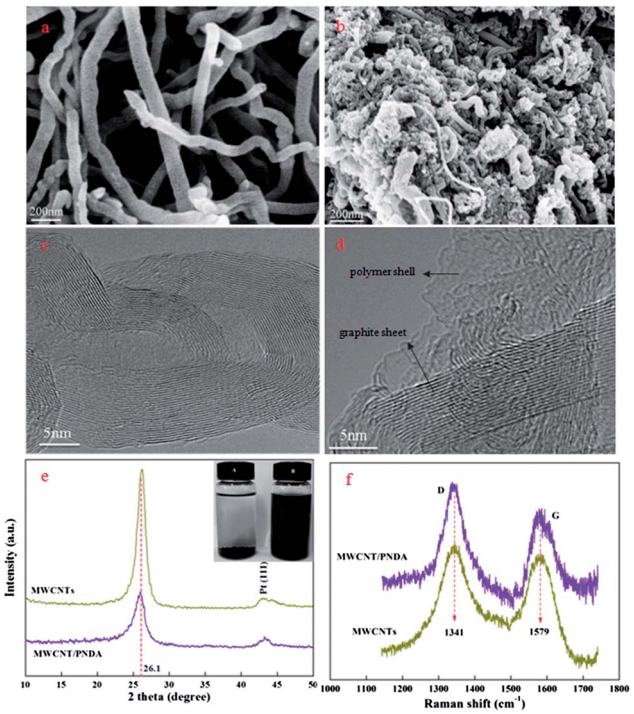

Fig. 1 SEM images of MWCNT (a) and MWCNT/PNDA (b); HR-TEM image of MWCNT (c) and MWCNT/PNDA (d); XRD patterns (e) and Raman spectra (f) of MWCNTs and MWCNT/PNDA. The inset figure of (e) shows a comparison of aqueous dispersion properties of MWCNTs (bottle A) imaged after 1 hour and MWCNT/PNDA (bottle B) imaged after 2 months.

1341 cm^{-1} is the D mode corresponding to the defects of the disordered sp^2-hybridized carbon atoms of nanotubes, sp^3 carbon, or other impurities. The peak near 1579 cm^{-1} is the G-band indicating the structural integrity of sp^2-hybridized carbon atoms of nanotubes.[21] Together, these bands can be used to evaluate the extent of carbon-containing defects. As can be observed, the values of I_G/I_D ratio are 0.95 for MWCNTs and 0.71 for MWCNT/PNDA, which correspond to the peak area of the Lorentzian functions to estimate the relative extent of structural defects. The I_G/I_D ratio value of MWCNTs decreases markedly after surface modification with PNDA, indicating the PNDA is grafted on the surface of MWCNTs. These results suggest that the MWCNT/PNDA composites are well synthesized and have more defects, which are benefit for the adsorption of metal ions. Chen *et al.*[9] had also reported that the plasma treatment can increase the surface defects of MWCNTs. The plasma technique has been shown to be effective in the surface modification of MWCNTs.

The nitrogen adsorption–desorption isotherms and pore size distribution of MWCNTs and MWCNT/PNDA are presented in Fig. 2a and b. The inset of Fig. 2a is the magnified part ($0.05 < P/P_o < 0.35$) of the isotherms. The adsorption isotherms show a slight adsorption in the low pressure region (<0.2 P/P_o) and no knee point appearance at low P/P_o, which means the interaction of adsorbent with adsorbate is very weak. As the P/P_o increasing, the adsorption also increases. It indicates there are some pores of adsorbent have been filled. The pore size of MWCNTs and MWCNT/PNDA determined in Fig. 2b are both in the mesopore range. According to N_2-BET measurements (Fig. 2a), the specific surface areas are 71.29 $m^2\ g^{-1}$ for raw MWCNTs and 108.5 $m^2\ g^{-1}$ for MWCNT/PNDA. Compared with MWCNTs, the specific surface area of the MWCNT/PNDA has increased by 53.67% after modification. All of these results may be due to the improvement of the dispersion, which prevents the aggregation of MWCNTs and increases the surface defects on the surface of MWCNT/PNDA. The higher surface area after grafting PNDA indicates the extension of the active surface for adsorption. Subsequently, more efficient utilization of the respective adsorption sites could be achieved in these new sorbents. To sum up, the MWCNT/PNDA composites could be a good candidate as sorbent.

The thermal degradation of composites was measured using a thermogravimetric analysis. Fig. 2c shows the TGA traces of MWCNT and MWCNT/PNDA under nitrogen. MWCNT shows only about 1.1% weight loss up to 500 °C due to the pyrolysis of the amorphous carbon and carbon impurity.[15] Therefore, the carbon impurity in MWCNTs used in the experiments is negligible. The weight loss corresponding to the pristine purified MWCNTs and MWCNT/PNDA at 800 °C under nitrogen is 4.4 and 12.0 wt%, respectively. The weight loss of MWCNTs in the range of 500–800 °C is due to the decomposition of functional groups such as carboxyl and hydroxyl groups.[23] For the sample of MWCNT/PNDA, the weight loss is likely due to the decomposition of grafted PNDA, suggesting that about 12 wt% PNDA is incorporated in MWCNT/PNDA composites. TGA analysis gives further evidence that PNDA is successfully grafted on the surfaces of MWCNTs.

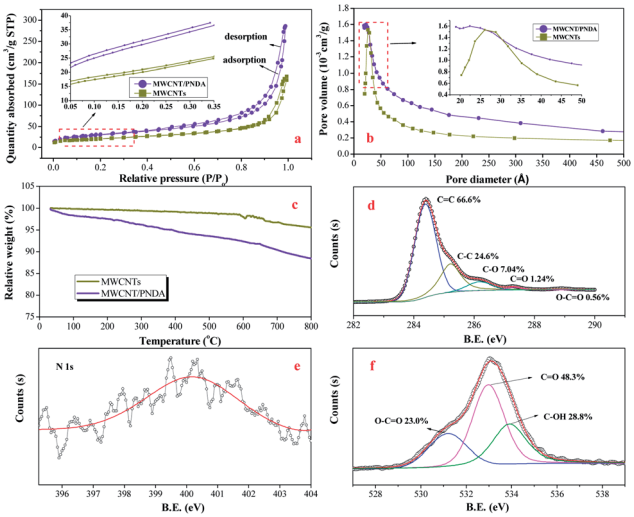

Fig. 2 Nitrogen adsorption–desorption isotherms (a); pore size distribution of MWCNTs and MWCNT/PNDA at 77.35 K (b); TGA curves of MWCNTs and MWCNT/PNDA in N_2 (c); XPS C 1s spectrum (d), N 1s spectrum (e), and O 1s spectrum (f) of MWCNT/PNDA.

In order to verify the above viewpoint, the element characterization of sample is analyzed by XPS (Fig. 2d–f). The spectra of XPS exist the characteristic peaks of N1s (400.1 eV) and O 1s, indicating the effective connection of PNDA onto MWCNTs. The C1s spectra (Fig. 2d) have characteristic peaks of C=C (284.4 eV), C–C (285.4 eV), C–O (286.2 eV), C=O (287.3 eV) and COO^- (288.9 eV),[24] which correspond to the existence of some hydroxyl (–C–OH), carboxyl (–COO^-), and carbonyl groups (>C=O). The O 1s spectrum (Fig. 2f) can be deconvoluted into three components: the peaks at 531.2 ± 0.2 eV, 532.8 ± 0.2 eV and 533.8 ± 0.2 eV are attributed to –COO^-, C=O and –C–OH species,[25] respectively. The results of O 1s are consistent with that of C 1s. From the XPS analysis, one can see that some of amide and oxygen-containing functional groups are on the surface of MWCNT/PNDA. Hence, Co(II) sorption on MWCNT/PNDA is probably through a surface sorption mechanism *via* coordination of Co d-electron to C=C (π-electrons) bond, –O–Co and –N–Co bond.

3.2 Potentiometric titration

The surface charge properties of adsorbent are fundamental and crucial, because they determine the adsorbent surface electrical charge from the reactions of adsorbent functional groups with adsorptive heavy metal ions in aqueous solution.[21] It can be investigated by potentiometric titration experiments. Potentiometric titration can provide a measure of the sequential binding of the proton by the surface functional groups of materials.[26] Herein, MWCNT and MWCNT/PNDA were characterized by potentiometric titration.

The potentiometric titration results of MWCNTs and MWCNT/PNDA are shown in Fig. 3. As can be seen from the potentiometric titration curves (Fig. 3a), the pH value jump of MWCNT/PNDA is much softer than that of MWCNTs, which means that the buffer capacity of MWCNT/PNDA is much

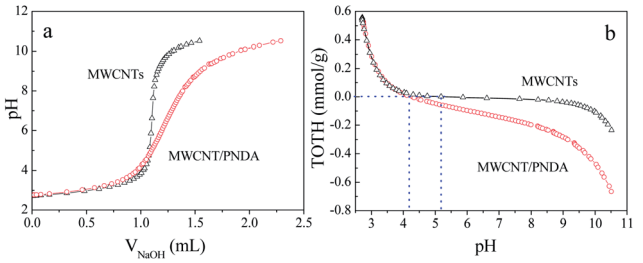

Fig. 3 Potentiometric titration curves (a) and TOTH curves (b) of MWCNTs and MWCNT/PNDA suspension with $m/V = 4.00$ g L^{-1}, $I = 0.01$ mol L^{-1} $NaClO_4$.

higher than that of MWCNTs. The amide functional groups of the PNDA grafted on MWCNT/PNDA surface can act as proton receivers in the potentiometric titration process, which improve its buffering capacity. And the further proof was confirmed from the TOTH curves in Fig. 3b.

TOTH is the total concentration of consumed protons in the titration process, which is calculated from the following equation:[26]

$$\mathrm{TOTH} = \frac{-(V_{\mathrm{NaOH}} - V_{\mathrm{eb1}})C_{\mathrm{NaOH}}}{V_0 + V_{\mathrm{at}} + V_{\mathrm{NaOH}}} \quad (3)$$

where V_0 is the initial volume of sorbent suspension; V_{eb1} is the volume of NaOH added in titration at Gran point to zero at acidic side; V_{at} is the total volume of added acid solution.

The titration curves of TOTH *vs.* pH for MWCNTs and MWCNT/PNDA are shown in Fig. 3b. At pH < 5.2, the surfaces of MWCNTs were positively charged, and at pH > 5.2, the surfaces of MWCNTs were negatively charged. However, at pH < 4.3, the surfaces of MWCNT/PNDA were positively charged, and at pH > 4.3, the surfaces of MWCNT/PNDA were negatively charged. The grafting of PNDA on the surfaces of MWCNTs decreases the point of zero change (pH_{pzc}) from 5.2 to 4.3.

3.3 Effect of environmental conditions on Co(II) sorption

The initial solution pH is an important parameter in metal ion sorption process, which affects both the dissociation degree of functional groups from the sorbent surface and the species of metal ions in aqueous solutions. The pH effect of Co(II) sorption on various kinds of sorbents had been studied extensively,[1,27–30] and the results indicated the solution pH exerted a pronounced effect on the uptake of Co(II) to solid particles. Fig. 4a shows the pH-dependence of Co(II) sorption on MWCNT/PNDA in different $NaClO_4$ concentrations. The sorption of Co(II) increases gradually in the pH range from 2.0 to 9.0, and then maintains the maximum sorption percentage of ~90% at pH 9.0–11.0. Further increase the pH does not benefit the removal of Co(II) from the solution. The results are similar to the sorption of Co(II) on goethite,[29] bentonite[30] and TiO_2.[28]

The observed pH-dependence of Co(II) sorption on MWCNT/PNDA may stem from cation exchange and the surface properties of MWCNT/PNDA, such as the surface charge and the protonation states of functional groups. As seen in Fig. 4a, at low pH (pH < 5) the highly concentrated hydronium ions are

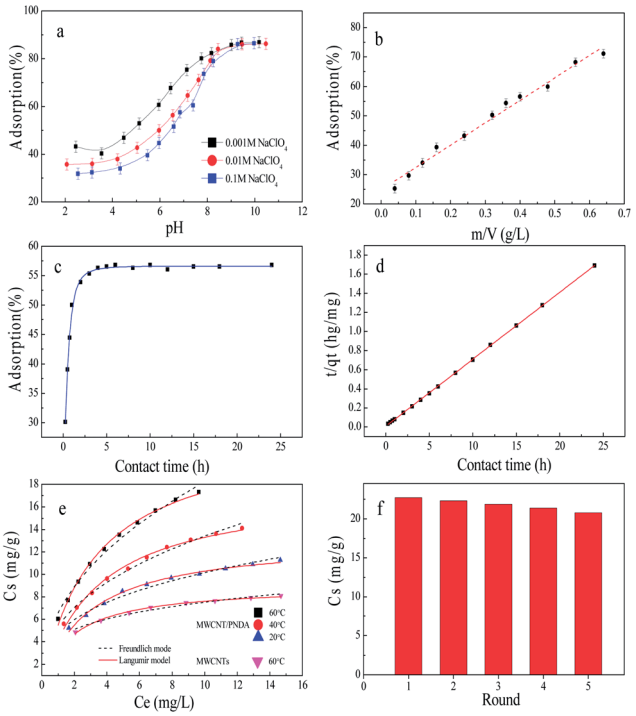

Fig. 4 Effect of pH and ionic strength (a); MWCNT/PNDA content (b); contact time (c); and the pseudo-second-order rate equation fit (d) of Co(II) onto MWCNT/PNDA, at pH = 6.5 ± 0.3, $T = 30 \pm 2$ °C, $C_{[Co(II)]initial} = 10.0$ mg L^{-1}, $I = 0.01$ M $NaClO_4$, $m/V = 0.4$ g L^{-1}. Adsorption isotherms of MWCNTs and MWCNT/PNDA at three different temperatures (e) and recyclable times of MWCNT/PNDA at $T = 60 \pm 2$ °C (f), with pH = 6.5 ± 0.3, $I = 0.01$ M $NaClO_4$, $m/V = 0.4$ g L^{-1}.

able to compete with Co^{2+} bound to the hydrophilic groups of MWCNT/PNDA, leading to a low Co^{2+} sorption on MWCNT/PNDA. In addition, the surface of MWCNT/PNDA contains a large number of binding sites, which are positively charged at low pH due to the surface protonation reaction. At low pH, Co^{2+} is the predominant Co(II) species.[29] And the electrostatic repulsion occurred between Co^{2+} and the positive charge on MWCNT/PNDA surface also leads to the low sorption percentage. The increase of pH suppresses the existence of hydronium and enhances the possibility of the MWCNT/PNDA active sites to be deprotonated, thus enhances the availability of negatively charged groups with Co(II) ions. In addition, before adding Co(II) ions, the Na^+ ions have equilibrated with MWCNT/PNDA and the sorption of Co(II) can be considered as the exchange of Co^{2+} with Na^+ ions. Moreover, as more surface functional groups are dissociated at high pH values than that at low pH values, more sorption sites are available for binding Co(II) ions. At pH 8.5–12, the predominant species of Co(II) are $Co(OH)^+$ and $Co(OH)_2$,[29] and they are easily to be adsorbed on the negatively charged MWCNT/PNDA surfaces. As a result, the maximum sorption of Co(II) is achieved at high level. According to the solubility constant (K_{sp}) of $Co(OH)_2$ (1.58×10^{-15}), and the Co(II) initial concentration of 10 mg L^{-1}, the pH value of appearance of the hydroxyl complexes precipitation is calculated to be 8.48. However, more than 70% Co(II) ions are adsorbed on MWCNT/PNDA at pH 8. Thereby it is impossible to

form precipitate because of the low concentration of Co(II) remained in aqueous solution. Therefore, the sorption of Co(II) on MWCNT/PNDA is not attributed to the precipitation of $Co(OH)_2(s)$ at high pH values.

The effect of background electrolyte concentrations on Co(II) sorption in a wide pH range is also shown in Fig. 4a. One can see that the sorption of Co(II) on MWCNT/PNDA at pH < 9.0 is influenced by ionic strength obviously, whereas no drastic difference of Co(II) sorption is found at pH > 9.0 in the three different $NaClO_4$ solution concentrations. The results of the effect of ionic strength on Co(II) sorption are consistent with previously results.[1,30] The ionic strength can influence the double electrode layer thickness and interface potential of solid particles, thereby can affect the binding of the adsorbed species. Outer-sphere surface coordination is more impressionable to ionic strength variations than inner-sphere surface coordination as the background electrolyte ions are placed in the same plane for outer-sphere surface complexes.[14] Thereby, the sorption of Co(II) on MWCNT/PNDA may imply the formation of outer-sphere surface complexes. Combined with the results of pH and ionic strength-dependent sorption, one can consider that there are two mechanisms for Co(II) sorption on MWCNT/PNDA: cation exchange and outer-sphere surface coordination, especially the strong surface coordination with the amide and oxygen-containing functional groups on the surfaces of MWCNT/PNDA.

Solid content is also an import part for the sorption of Co(II) (Fig. 4b). The removal of Co(II) obviously increases with increasing solid content. With increasing solid content, the number of available functional groups at the MWCNT/PNDA surfaces increases. Consequently, more efficient utilization surface sites are available to form complexes with Co(II) at solid surfaces, and thereby enhances Co(II) sorption on MWCNT/PNDA composites.

Fig. 4c shows the sorption of Co(II) to MWCNT/PNDA as a function of contact time. A rapid sorption occurs at the first contact time of 3 h and then remains constant with increasing contact time. The pseudo-second-order model was proved to be the best correlation for the kinetic sorption processes.[1,31]

$$\frac{t}{q_t} = \frac{1}{2K'q_e^2} + \frac{t}{q_e} \quad (4)$$

where K' (g mg^{-1} h^{-1}) is the pseudo-second-order rate constant of adsorption, q_t (mg g^{-1}) is the amount of Co(II) adsorbed on the sorbent at time t (min), and q_e (mg g^{-1}) is the equilibrium sorption capacity. Linear plot feature of t/q_t *vs.* t is achieved and showed in Fig. 4d. The K' value calculated from the slope and intercept is 0.26 g mg^{-1} h^{-1}. The correlation coefficient R (R = 0.999) for the linear plot is very close to 1, which suggests that the kinetic sorption can be well described by the pseudo-second-order rate equation.

The sorption isotherms of Co(II) on MWCNT/PNDA obtained at 20, 40 and 60 °C are shown in Fig. 4e. The sorption isotherm is the highest at T = 60 °C and is the lowest at T = 20 °C. The results indicate that high temperature is advantageous for Co(II) sorption on MWCNT/PNDA. Thus, the sorption process of Co(II) is endothermic. In order to understand the sorption mechanism, Langmuir[14] ($C_s = C_{smax}K_LC_e/(1 + K_LC_e)$, C_{smax} (mg g^{-1}) is the maximum sorption capacity and K_L (L mg^{-1}) is the Langmuir adsorption constant) and Freundlich[14] ($C_s = K_FC_e^{1/n}$, K_F (mg^{1-n} L^n g^{-1}) and $1/n$ are the constants) equilibrium isotherm models are conducted to fit the experimental data. The Langmuir model assumes monolayer coverage on adsorbent, while the Freundlich model allows for multilayer adsorption on adsorbent. The Langmuir and Freundlich isotherm parameters calculated from the sorption isotherms are listed in Table 1.

One can see that the Langmuir model fits the experiment data a little better than the Freundlich one. Comparing to MWCNT/PNDA, the adsorption capacity of the pristine MWCNTs was also investigated (Fig. 4e). The two curves resemble the same trend; however, the adsorption for MWCNT/PNDA is much higher than that for pristine MWCNTs. It can be calculated that the maximum sorption capacity (C_{smax}) of Co(II) on MWCNT/PNDA is 22.78 mg g^{-1} (pH = 6.5 and T = 60 °C), which is about 2.5 times higher than that of MWCNTs (9.02 mg g^{-1}) and 2 times higher than that of oxidized MWCNTs (10.74 mg g^{-1}, pH = 6.4 and T = 70 °C).[27] The enhanced sorption of Co(II) on MWCNT/PNDA is due to the strong surface coordination of Co(II) ions with the amino groups on the surfaces of MWCNT/PNDA and the significant change of physical properties such as the specific surface area and pore volume distribution. Otherwise, sorption capacities of Co(II) on various sorbents collected from the references are listed in Table 2. The comparative results show that the sorption capacity of MWCNT/PNDA is higher than that of a number of other sorbents. Besides the large surface area, the amide and oxygen-containing functional groups also play important parts in the efficient

Table 1 The parameters of MWCNT/PNDA for the Langmuir and Freundlich models at different temperatures

	Langmuir			Freundlich		
T (°C)	C_{smax} (mg g^{-1})	K_L (L mg^{-1})	R^2	n	K_F (mmol g^{-1})	R^2
20	13.18	0.36	0.992	3.03	4.74	0.978
40	17.73	0.30	0.993	2.49	5.32	0.988
60	22.78	0.32	0.996	2.25	6.54	0.989

Table 2 Comparison of maximum sorption capacity for Co(II) by various sorbents

Sorbents	Conditions	C_{smax} (mg g^{-1})	Ref.
MWCNTs	pH 6.5, 60 °C	9.02	This work
Goethite	pH 6.8, 70 °C	9.84	27
Oxidized MWCNT	pH 6.4, 70 °C	10.74	25
Neutral zeolite	pH 6–7, 25 °C	14.38	30
Magnetite/graphene oxide	pH 6.8, 70 °C	22.70	1
MWCNT/PNDA	pH 6.5, 60 °C	22.78	This work
Bi-montmorillonite	pH 6.0, 70 °C	31.04	31
TiO_2/eggshell	pH 7.0, 70 °C	33.90	26

utilization of sorption sites of MWCNT/PNDA. The greater maximum sorption capacity of Bi-montmorillonite and TiO_2/eggshell may be due to the cation exchange capacity played a more important role in this case. Although the adsorption capacity of MWCNT/PNDN composites is lower than that of Bi-montmorillonite and TiO_2/eggshell, the synthesis procedure of MWCNT/PNDN composites is more time-efficient and facile than that of the other two materials and no need to heat at 500 °C. Therefore, MWCNT/PNDN composites can be one of novel adsorbent materials.

The recyclability is an important factor for an advanced adsorbent. The recyclable times of MWCNT/PNDA composites for the removal of Co(II) were investigated (Fig. 4f). After adsorption, desorption was carried out by washing out MWCNT/PNDA bounded Co(II) with HNO_3 (pH ~ 2). The suspension was then washed several times with Milli-Q water, dried in a vacuum oven at 80 °C, and finally the MWCNT/PNDA composites were reused. Fig. 4f shows that after 5 cycles the adsorption capacity of Co(II) decreases slightly by 8% from 22.7 mg g^{-1} to 20.8 mg g^{-1}, indicating a good chemical stability and reusability.

3.4 Thermodynamic analysis

The distribution coefficients (K_d) and the thermodynamic parameters (ΔH^0, ΔS^0, and ΔG^0) for Co(II) sorption on MWCNT/PNDA can be determined from the temperature dependent sorption isotherms. The free energy change (ΔG^0) and K_d are calculated from the following equations:

$$\Delta G^0 = -RT \ln K^0 \quad (5)$$

$$K_d = \frac{(C_0 - C_e)}{C_e} \times \frac{V}{M} \quad (6)$$

where K^0 is the sorption equilibrium constant. Values of $\ln K^0$ are obtained by plotting $\ln K_d$ *versus* C_e and extrapolating C_e to zero. Standard entropy change (ΔS^0) and the average standard enthalpy change (ΔH^0) are calculated using the equations:

$$\Delta S^0 = -\left(\frac{\partial G^0}{\partial T}\right)_P \quad (7)$$

$$\Delta H^0 = \Delta G^0 + T\Delta S^0 \quad (8)$$

Table 3 lists the thermodynamic parameters calculated from the adsorption isotherms at pH = 6.5 at three different temperatures. The determination of thermodynamic parameters provides an insight into the mechanism concerning the adsorptive interaction of Co(II) with MWCNT/PNDA. The positive value of ΔH^0 indicates that the sorption is endothermic, and it is consistent with the increasing sorption as the temperature increases. This is due to the solvent effect for Co(II) appears as hydrated species in aqueous phase. The sorption of Co(II) is thus at the cost of breaking interactions between Co(II) and one or some coordinated water molecules, which needs energy and high temperature. The results indicate that the energy absorbed in the desolvation process is higher than the adsorption enthalpy. The negative value of ΔG^0 expected as a spontaneous process under the conditions applied. The value of ΔG^0 becomes more negative with the increase of temperature, indicating more efficient sorption at high temperature. At higher temperature, more coordinated water molecules break from the Co(II), resulting in more rest coordination sites to the sorption on the sorbent. The positive value of ΔS^0 also indicates the spontaneous sorption process and reflects the affinity of MWCNT/PNDA toward Co(II) ions in aqueous solutions.

Table 3 Values of thermodynamic parameters for Co(II) sorption on MWCNT/PNDA

T (°C)	ΔG^0 (kJ mol^{-1})	ΔS^0 (J mol^{-1} K^{-1})	ΔH^0 (kJ mol^{-1})
20	−19.19	109.2	12.82
40	−21.26		12.94
60	−23.56		12.82

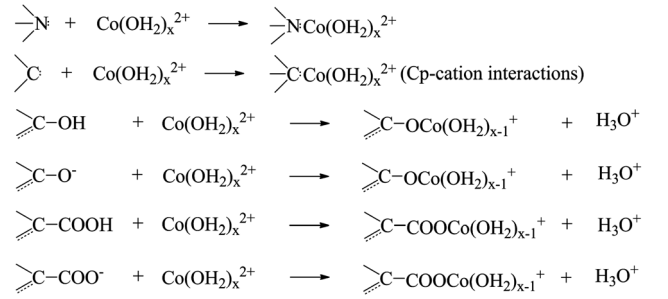

Fig. 5 The possible coordination sorption mechanisms of Co(II) on MWCNT/PNDA.

3.5 Mechanisms of Co(II) sorption on MWCNT/PNDA

Combined with the characterization and batch experimental investigations, cation exchange and outer-sphere surface coordination are considered as the two mechanisms for Co(II) sorption on MWCNT/PNDA. And the coordination of Co d-electron with amide and oxygen-containing functional groups (*e.g.*, hydroxyl, carboxyl, and epoxy) or C=C (π-electrons) bond have been proposed to be the major mechanisms for Co(II) sorption on MWCNT/PNDA. Considering the deprotonated state, the possible coordination sorption mechanisms can be described schematically as Fig. 5.

4. Conclusions

In summary, we have developed a two-step method to improve the dispersion and adsorption properties of CNTs in aqueous solution. Based on the results mentioned above, the following conclusions can be drawn:

(1) The MWCNT/PNDA composites have excellent dispersion property and high-efficient properties in the preconcentration and separation of Co(II) ions from aqueous solutions.

(2) The sorption of Co(II) ions on MWCNT/PNDA composites strongly depends on pH values, ionic strength and temperature.

The neutral and basic condition with low ionic strength and high temperature is benefit to the sorption process.

(3) The coordination of Co d-electron with amide and oxygen-containing functional groups (*e.g.*, hydroxyl, carboxyl, and epoxy) or C=C (π-electrons) bond have been proposed to be the major mechanisms for Co(II) ions sorption by MWCNT/PNDA.

(4) The creation of PNDA-coated MWCNTs opens up a wide range of novel applications for CNTs, particularly in the field of the wastewater treatment.

Acknowledgements

We are grateful to Dr Raman Bekarevich of Shizuoka University for the high resolution transmission electron microscopy measurement. This work has been supported in part by the National Natural Science Foundation of China (21225730; 21272236).

Notes and references

1 M. C. Liu, C. L. Chen, J. Hu, X. L. Wu and X. K. Wang, *J. Phys. Chem. C*, 2011, **115**, 25234–25240.
2 W. F. Du, L. Wilson, J. Ripmeester, R. Dutrisac, B. Simard and S. Denommee, *Nano Lett.*, 2002, **2**, 343–346.
3 S. Iijima, *Nature*, 1991, **354**, 56–58.
4 R. Q. Long and R. T. Yang, *J. Am. Chem. Soc.*, 2001, **123**, 2058–2059.
5 T. Premkumar, R. Mezzenga and K. E. Geckeler, *Small*, 2012, **8**, 1299–1313.
6 C. Gao, H. He, L. Zhou, X. Zheng and Y. Zhang, *Chem. Mater.*, 2009, **21**, 360–370.
7 C. Gao, C. D. Vo, Y. Z. Jin, W. W. Li and S. P. Armes, *Macromolecules*, 2005, **38**, 8634–8648.
8 X. Lou, C. Detrembleur, C. Pagnoulle, R. Jérôme, V. Bocharova, A. Kiriy and M. Stamm, *Adv. Mater.*, 2004, **16**, 2123–2127.
9 C. L. Chen, A. Ogino, X. K. Wang and M. Nagatsu, *Appl. Phys. Lett.*, 2010, **96**, 131504.
10 S. Das, A. S. Wajid, J. L. Shelburne, Y. C. Liao and M. J. Green, *ACS Appl. Mater. Interfaces*, 2011, **3**, 1844–1851.
11 G. P. Rao, C. Lu and F. Su, *Sep. Purif. Technol.*, 2007, **58**, 224–231.
12 X. M. Ren, C. L. Chen, M. Nagatsu and X. K. Wang, *Chem. Eng. J.*, 2011, **170**, 395–410.
13 X. Y. Yu, T. Luo, Y. X. Zhang, Y. Jia, B. J. Zhu, X. C. Fu, J. H. Liu and X. J. Huang, *ACS Appl. Mater. Interfaces*, 2011, **3**, 2585–2593.
14 S. B. Yang, J. Hu, C. L. Chen, D. D. Shao and X. K. Wang, *Environ. Sci. Technol.*, 2011, **45**, 3621–3627.
15 D. D. Shao, Z. Q. Jiang, X. K. Wang, J. X. Li and Y. D. Meng, *J. Phys. Chem. B*, 2009, **113**, 860–864.
16 D. D. Shao, J. Hu and X. K. Wang, *Plasma Processes Polym.*, 2010, **7**, 977–985.
17 M. V. Naseh, A. A. Khodadadi, Y. Mortazavi, F. Pourfayaz, O. Alizadeh and M. Maghrebi, *Carbon*, 2010, **48**, 1369–1379.
18 B. P. Grady, *Macromol. Rapid Commun.*, 2010, **31**, 247–257.
19 Z. Jia, Q. Fu and J. Huang, *Macromolecules*, 2006, **39**, 5190–5193.
20 F. M. Blighe, Y. R. Hernandez, W. J. Blau and J. N. Coleman, *Adv. Mater.*, 2007, **19**, 4443–4447.
21 D. D. Shao, X. M. Ren, J. Hu, Y. X. Chen and X. K. Wang, *Colloids Surf., A*, 2010, **360**, 74–84.
22 D. Xu, X. L. Tan, C. L. Chen and X. K. Wang, *J. Hazard. Mater.*, 2008, **154**, 407–416.
23 S. Chen, G. Wu, Y. Liu and D. Long, *Macromolecules*, 2005, **39**, 330–334.
24 S. B. Yang, X. L. Wu, C. L. Chen, H. L. Dong, W. P. Hu and X. K. Wang, *Chem. Commun.*, 2012, **48**, 2773–2775.
25 G. X. Zhao, D. D. Shao, C. L. Chen and X. K. Wang, *Appl. Phys. Lett.*, 2011, 98.
26 X. M. Ren, J. X. Li, X. L. Tan and X. K. Wang, *Dalton Trans.*, 2013, **42**, 5266–5274.
27 Q. Wang, L. Chen and Y. B. Sun, *J. Radioanal. Nucl. Chem.*, 2012, **291**, 787–795.
28 S. W. Zhang, H. H. Niu, Z. Q. Guo, Z. S. Chen, H. P. Wang and J. Z. Xu, *J. Radioanal. Nucl. Chem.*, 2011, **289**, 479–487.
29 Z. Q. Guo, D. P. Xu, D. L. Zhao, S. W. Zhang and J. Z. Xu, *J. Radioanal. Nucl. Chem.*, 2011, **287**, 505–512.
30 W. M. Dong, X. K. Wang, Y. Shen, X. D. Zhao and Z. Y. Tao, *J. Radioanal. Nucl. Chem.*, 2000, **245**, 431–434.
31 Y. S. Ho and G. McKay, *Process Biochem.*, 1999, **34**, 451–465.